J Mol Med (2013) 91:759–770
DOI 10.1007/s00109-013-0995-3

JMolMed

ORIGINAL ARTICLE

Single-stranded nucleic acids promote SAMHD1 complex formation

Victoria Tüngler · Wolfgang Staroske · Barbara Kind · Manuela Dobrick · Stefanie Kretschmer · Franziska Schmidt · Claudia Krug · Mike Lorenz · Osvaldo Chara · Petra Schwille · Min Ae Lee-Kirsch

Received: 19 October 2012 / Revised: 3 December 2012 / Accepted: 2 January 2013 / Published online: 31 January 2013

Abstract SAM domain and HD domain-containing protein 1 (SAMHD1) is a dGTP-dependent triphosphohydrolase that degrades deoxyribonucleoside triphosphates (dNTPs) thereby limiting the intracellular dNTP pool. Mutations in SAMHD1 cause Aicardi–Goutières syndrome (AGS), an inflammatory encephalopathy that mimics congenital viral infection and that phenotypically overlaps with the autoimmune disease systemic lupus erythematosus. Both disorders are characterized by activation of the antiviral cytokine interferon-α initiated by immune recognition of self nucleic acids. Here we provide first direct evidence that SAMHD1 associates with endogenous nucleic acids in situ. Using fluorescence cross-correlation spectroscopy, we demonstrate that SAMHD1 specifically interacts with ssRNA and ssDNA and establish that nucleic acid-binding and formation of SAMHD1 complexes are mutually dependent. Interaction with nucleic acids and complex formation do not require the SAM domain, but are dependent on the HD domain and the C-terminal region of SAMHD1. We finally demonstrate that mutations associated with AGS exhibit both impaired nucleic acid-binding and complex formation implicating that interaction with nucleic acids is an integral aspect of SAMHD1 function.

Keywords SAMHD1 · Aicardi–Goutières syndrome · Fluorescence cross-correlation spectroscopy · Nucleic acids

Victoria Tüngler and Wolfgang Staroske joint first authorship.

Electronic supplementary material The online version of this article (doi:10.1007/s00109-013-0995-3) contains supplementary material, which is available to authorized users.

V. Tüngler · B. Kind · M. Dobrick · S. Kretschmer · F. Schmidt · C. Krug · M. A. Lee-Kirsch (✉)
Children's Hospital, Technical University Dresden,
01307 Dresden, Germany
e-mail: minae.lee-kirsch@uniklinikum-dresden.de

W. Staroske · P. Schwille
Biotechnology Center, Technical University Dresden,
01307 Dresden, Germany

M. Lorenz
Max Planck Institute of Molecular Cell Biology and Genetics,
01307 Dresden, Germany

O. Chara
Center for Information Services and High Performance Computing, Technical University Dresden,
01062 Dresden, Germany

O. Chara
Institute of Physics of Liquids and Biological Systems (IFLYSIB),
CONICET, National University of La Plata,
B1900BTE La Plata, Argentina

P. Schwille
Max Planck Institute of Biochemistry,
82152 Martinsried, Germany

Introduction

SAMHD1 (SAM domain and HD domain-containing protein 1) functions as a dGTP-dependent phosphohydrolase which converts deoxynucleoside triphosphates (dNTPs) to the constituent deoxynucleoside and inorganic triphosphate [1]. SAMHD1 was recently identified as a factor that restricts infection of myeloid cells with human immunodeficiency virus type 1 (HIV-1) by depleting the dNTP pool required for reverse transcription of the viral RNA genome [2–4]. Mutations of SAMHD1 cause Aicardi–Goutières syndrome (AGS), an inflammatory encephalopathy [5]. AGS is also caused by mutations in the genes encoding the 3′-repair exonuclease (TREX1) and the RNase H2 complex (RNASEH2A-C) [6, 7]. The phenotype of AGS overlaps with the autoimmune disease systemic lupus erythematosus (SLE) [8, 9]. Mutations in SAMHD1 and TREX1 also cause

familial chilblain lupus [10–12], and TREX1 variants confer a high risk for developing SLE [13], highlighting the role of nucleic acid metabolism in mechanisms of immune tolerance.

Although the association of SAMHD1 with AGS has established its role as negative regulator of the innate immune response [5], the mechanisms underlying SAMHD1 deficiency remain largely undefined. Given the role of self-nucleic acids in the pathogenesis of systemic autoimmunity, we investigated the nucleic acid-binding properties of SAMHD1. Here we provide further insight into the physiological role of SAMHD1 by showing that it associates with single-stranded nucleic acids and forms complexes of higher order. AGS-associated mutations exhibit both impaired nucleic acid-binding and complex formation implicating that SAMHD1 function is dependent on its interaction with nucleic acids.

Materials and methods

Constructs

N-terminally GFP-tagged wild-type SAMHD1 (GFP-SAMHD1) and deletion mutants (GFP-SAMHD1$_{1-130}$, GFP-SAMHD1$_{111-626}$) were cloned into pEGFP-C1 (Clontech). SAMHD1 mutations identified in AGS patients (H167Y, R290H, Q548X) were introduced by site-directed mutagenesis (QuikChange Lightning). GFP was replaced by mCherry using AgeI and BsrGI.

Fluorescence lifetime imaging microscopy

In situ interaction of GFP-SAMHD1 with nucleic acids was determined by fluorescence lifetime imaging microscopy using the fluorescent nucleic acid stain Sytox Orange (Molecular Probes) as described previously [14]. HeLa cells grown on coverslips were transfected with GFP-SAMHD1-plasmid using FuGENE HD (Roche Diagnostics). Cells were fixed in 4 % paraformaldehyde and permeabilized with PBS-Triton (0.5 %). Nucleic acids were digested with 20 U/ml DNase I (Applied Biosystems) or 0.1 mg/ml RNase A (QIAgen) at 37 °C for 30 min. Cells were stained for 30 min with 5 μM Sytox Orange, washed three times with PBS-Tween (0.2 %) and mounted with Vectashield HardSet Mounting Medium (Vector Labs).

Fluorescent cross-correlation spectroscopy

For FCCS experiments in cell lysates, HEK293 cells were transfected with GFP-SAMHD1 and mCherry-constructs using polyethylenimine. Cells were lysed in lysis buffer (137 mM NaCl, 12 mM phosphate, 2.7 mM KCl, 4 mM $CaCl_2.6H_2O$, 0.8 mM EGTA, protease and phosphatase inhibitors) by sonication and shearing. Cellular debris was removed by centrifugation. For FCCS, 10 μMol of oligonucleotide labelled with 6-TAMRA at the 3′-end without further chemical modification (Metabion, Supplementary Table S1) were added to 45 μl freshly prepared lysate and measured immediately. Double-stranded oligonucleotides were prepared by heat denaturation followed by slow cooling to room temperature. Complete hybridization of oligonucleotides was confirmed by polyacrylamide gel electrophoresis. For analysis of complex formation, equal amounts of GFP- and mCherry-labelled molecules were achieved by count rate quantification prior to mixing of lysates and incubation over night at 21 °C. For FCCS experiments in living cells, HeLa cells were transfected with GFP-SAMHD1 and mCherry-SAMHD1-constructs using FuGENE HD (Roche Diagnostics).

FCCS permits probing the dynamic interactions of molecules labelled with two spectrally different fluorophors [15, 16]. Diffusion of fluorescent molecules through the focal spot induces fluorescence fluctuation. Both fluctuating fluorescence signals are subjected to auto-correlation analysis, and the cross-correlation function is obtained by correlating intensity fluctuations with each other. Only dual labelled molecules translocating through the detection volume contribute to the cross-correlation curve. Hence, the amplitude of the cross-correlation curve is directly proportional to the amount of double-labelled species and allows a quantitative analysis of interactions. FCCS was carried out as described in Supplementary Methods.

Pull-down assay

THP-1 cells were lysed in 4-(2-hydroxyethyl)-1-piperazineethanesulphonic acid (HEPES) buffer (20 mM HEPES, 4 mM $CaCl_2.6H_2O$, 0.8 mM EGTA, 150 mM NaCl, protease and phosphatase inhibitors), pre-cleared and incubated with 3′-biotinylated oligonucleotides (Supplementary Table S1) for 1 h at 4 °C. Samples were added to 25 μl of washed Dynabeads MyOne Streptavidin T1 (Invitrogen) and incubated overnight at 4 °C. Beads were washed ten times with PBS containing 2 %Triton-X and 0.2 mM NaCl and subjected to Western blotting using anti-SAMHD1-antibody.

Gel filtration chromatography

THP-1 cells were lysed in HEPES buffer. Aliquots containing 2.5 mg of total protein were incubated with or without 500 U of benzonase for 30 min at room temperature and size-fractionated by fast performance liquid chromotography using a Superose 6HR 10/30 column (Amersham Biosciences) equilibrated with HEPES buffer at 4 °C. Collected fractions were analysed by Western blotting using anti-SAMHD1-antibody. Mass standards including ovalbumin (43 kDa), catalase (240 kDa), ferritin (440 kDa) and thyroglobulin (669 kDa)

were run in parallel and used for calculation of a standard curve based on the elution volumes.

Immunofluorescence and Western blotting

HeLa transfected with GFP-SAMHD1 were fixed in 4 % paraformaldehyde, washed twice with PBS and mounted in Vectashield Mounting Medium with DAPI (Vector Labs). SAMHD1 in human fibroblasts was stained with mouse-anti-SAMHD1 (Sigma) followed by AlexaFluor 488 goat-anti-mouse-IgG (Invitrogen). Confocal microscopy was carried out on a Leica TCS SP5 II. For Western blotting, cell lysates were subjected to sodium dodecyl sulphate polyacrylamide gel electrophoresis (SDS-PAGE), transferred onto nitrocellulose membrane and incubated with rabbit-anti-SAMHD1 antibody (ProteintechGroup, Inc.) or mouse-anti-β-actin (Invitrogen) followed by HRP-conjugated donkey-anti-rabbit-IgG (GE Healthcare) or rabbit-anti-mouse IgG (Dako), respectively. Immunoreactive signals were detected by chemiluminescence (Roche LumiLight PLUS).

Results

SAMHD1 associates with nucleic acids in situ

In presence of Sytox Orange, the lifetime of GFP-SAMHD1 significantly decreased from 2.05±0.03 to 1.88±0.07 ns, while the life time of GFP alone was not affected (Fig. 1), indicating an energy transfer and thus interaction of SAMHD1 with nucleic acids. To determine which nucleic acid species is targeted by SAMHD1, cells were incubated with DNase I or RNase A, respectively, prior to staining with Sytox Orange (Supplementary Figure 1a). Preincubation with RNase A almost completely abolished the lifetime reduction of GFP-SAMHD1 in the presence of Sytox Orange (Fig. 1) indicating that SAMHD1 strongly interacts with RNA. Removal of DNA by DNase I led to a significant reduction of GFP-SAMHD1 lifetime that was not as pronounced as in cells without DNase I treatment demonstrating that SAMHD1 also interacts with DNA.

SAMHD1 specifically interacts with ssRNA and ssDNA

Using FCCS, we further examined the interaction of GFP-SAMHD1 with TAMRA-labelled oligonucleotides in cell lysates. GFP-SAMHD1 exhibited a strong cross-correlation with ssRNA (65±28 %) and ssDNA (46±13 %), while cross-correlation of GFP-SAMHD1 with dsRNA, dsDNA or RNA/DNA hybrids did not differ from background levels observed with GFP alone (Fig. 2a, b). To test whether endogenous SAMHD1 interacts with nucleic acids, pull-down assays were carried out in monocytic THP-1 cells using 3′-biotinylated oligonucleotides (Fig. 2c). Consistent with our FCCS data, endogenous SAMHD1 was pulled down with ssRNA and ssDNA, but not with dsRNA, dsDNA or RNA/DNA hybrids. Thus, SAMHD1 specifically targets single-stranded nucleic acids.

Interaction of SAMHD1 with ssRNA and ssDNA is disrupted by mutations from patients with Aicardi–Goutières syndrome

We next examined the effects of SAMHD1 mutations identified in AGS patients [5, 8, 9] on nucleic acid-binding (Fig. 2d). H167Y affects the first histidine of the HD domain and was found in the homozygous state. R290H affects a highly conserved residue within the HD domain region and was found along with Q548X in an AGS patient who also presented with SLE. In addition, two deletion mutants, one consisting of the N-terminal 130 amino acids containing the SAM domain (SAM; GFP-SAMHD1$_{1–130}$) and one lacking the SAM domain (ΔSAM; GFP-SAMHD1$_{111–626}$), respectively, were studied. As shown in Fig. 2e, all AGS-associated mutations as well as SAM greatly reduced cross-correlation with ssRNA and ssDNA. In contrast, ΔSAM displayed a cross-correlation similar to wild-type SAMHD1, indicating that the C-terminal part containing the HD domain is sufficient for nucleic acid-binding (Fig. 2e). Like wild-type SAMHD1, none of the AGS-associated SAMHD1 mutations showed cross-correlation with double-stranded nucleic acids (Supplementary Figure S2).

SAMHD1 forms complexes of higher order

The auto-correlation curves of GFP-SAMHD1 were shifted to a longer lag time τ compared to monomeric GFP consistent with a 2.7-fold slower diffusion (Fig. 2). Assuming globular molecules, the diffusion of GFP-SAMHD1 (99.1 kDa) would be expected to be only 1.5-fold slower than monomeric GFP (26.9 kDa) suggesting oligomerisation of SAMHD1. We therefore explored complex formation by FCCS. In cell lysates containing wild-type GFP-SAMHD1 and mCherry-SAMHD1, a strong cross-correlation of 79±14 % was observed indicating a high likelihood of SAMHD1 complexes of at least two monomers (Fig. 3a). Cross-correlation of a GFP-mCherry-fusion protein was approximately 45 % (data not shown) consistent with a dark fraction of mCherry of 55 to 60 % [17]. Therefore, the very high cross-correlation of 79 % for wild-type SAMHD1 could have only been achieved if more than two mCherry-SAMHD1 molecules were present in the complex with nearly no monomers left in the cell lysate mixture. No cross-correlation was observed in lysates containing monomeric GFP or mCherry mixed with mCherry-SAMHD1 or GFP-SAMHD1, respectively (Fig. 3a).

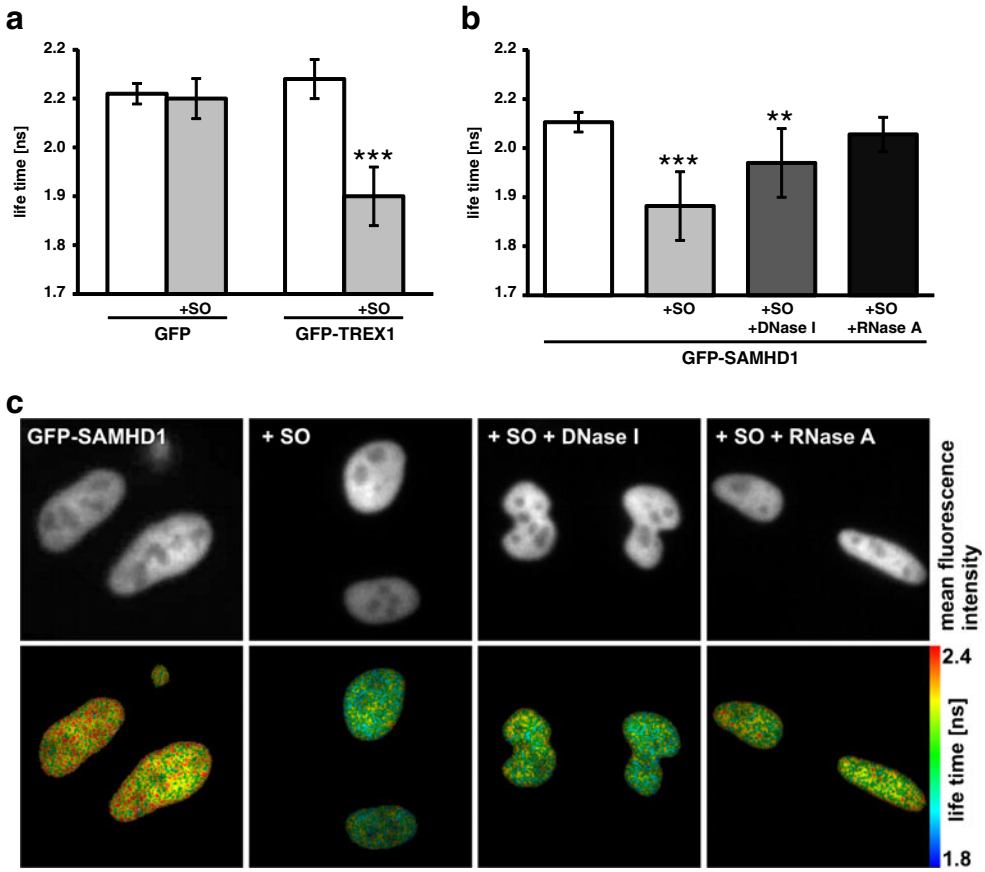

Fig. 1 Interaction of GFP-SAMHD1 with nucleic acids in situ. **a** Fluorescence lifetime of GFP and GFP-TREX1, a DNA exonuclease, expressed in HeLa cells in absence or presence of Sytox Orange (+ SO). The life time of GFP-TREX1 decreases significantly in the presence of Sytox Orange indicating interaction with nucleic acids. **b** Lifetime of GFP-SAMHD1 in absence or presence of Sytox Orange (+ SO) alone or after incubation with DNase I (+ SO+DNase I) or RNase A (+ SO+RNase A), respectively. A significant reduction of lifetime of GFP-SAMHD1 in presence of Sytox Orange indicates interaction with nucleic acids. This interaction is partially or completely lost after removal of DNA or RNA, respectively. Five to ten cells were measured per experiment. Data are presented as mean±SD of three independent experiments. $^{**}p<0.01$, $^{***}p<0.001$ versus GFP-TREX1 or GFP-SAMHD1 without Sytox Orange, unpaired Student's *t* test. **c** The *top row* shows the fluorescence intensity of HeLa cells expressing GFP-SAMHD1, and the *bottom row* shows the corresponding false colour-coded lifetime images

When we mixed each of the AGS-associated SAMHD1 mutants as GFP- and mCherry-tagged fusion proteins, respectively, cross-correlation significantly decreased to 10–30 %, consistent with impaired homomer formation (Fig. 3a). Likewise, cross-correlation of wild-type mCherry-SAMHD1 with either GFP-SAMHD1-H167Y, GFP-SAMHD1-R290H or GFP-SAMHD1-Q548X was significantly reduced, showing that wild-type mutant heteromer formation was also disturbed (Fig. 3a). Since all AGS-associated mutants carried an intact SAM-domain, these findings indicate that the SAM-domain is dispensable for oligomerisation. Indeed, ΔSAM showed a strong cross-correlation, demonstrating a preserved capability to oligomerise. In contrast, mutations affecting either the histidine of the HD domain (H167Y), the HD domain region (R290H) or the C-terminal end of SAMHD1 (Q548X), respectively, greatly impair oligomerisation. Thus, mutations that interfere with binding of SAMHD1 to nucleic acids also impair oligomerisation, indicating an important role of nucleic acid-binding for oligomerisation of SAMHD1.

To further characterize the composition of SAMHD1 complexes, we analysed the average brightness of GFP-SAMHD1 and mCherry-SAMHD1. In lysates with wild-type SAMHD1, the relative brightness of GFP-SAMHD1 in the complexes was on average 3.2-fold higher compared to monomeric GFP (Fig. 3b). In the same mixture, wild-type mCherry-SAMHD1 was 3.7-fold brighter than monomeric mCherry after correction for a dark fraction of 55 % [17, 18]. The correction formula and measured values are provided in Supplementary Methods and Supplementary Figure S3. The relative brightness values of ~3 to 4 represent the average overall particles sizes diffusing through the confocal volume. This means that within the distribution of

different oligomerisation states of SAMHD1, the average particle consists of eight SAMHD1 molecules (four GFP-SAMHD1 and four mCherry-SAMHD1). A conclusion about the width of this distribution, i.e. the smallest and the biggest complexes, cannot be drawn from the FCCS measurements. The average brightness values together with the very high cross-correlation would be consistent with a higher-ordered oligomeric configuration of SAMHD1 in cell lysates.

In agreement with the finding that the AGS-associated mutants were unable to oligomerise, their average brightness values were comparable to those of the monomeric fluorescent proteins (Fig. 3b). Similarly, the brightness of GFP-SAMHD1-R290H or GFP-SAMHD1-Q548X was comparable to that of monomeric GFP when mixed with mCherry-SAMHD1-Q548X or mCherry-SAMHD1-R290H, respectively. Like wild-type GFP-SAMHD1, GFP-ΔSAM displayed an average brightness of close to four GFP units demonstrating that is was also oligomerisation competent (Fig. 3b) and confirming that the SAM domain region is not required for complex formation.

We further assessed complex formation of endogenous SAMHD1 in THP-1 cells by gel filtration chromatography. As shown in Fig. 3c, SAMHD1 co-elutes over a molecular weight range from 70 to over 700 kDa. Following pretreatment of THP-1 lysate with benzonase, an endonuclease degrading DNA and RNA, SAMHD1 immunoreactivity in fractions of higher mass disappeared suggesting disassembly of higher-ordered complexes. Consistent with complex formation observed with FCCS, these findings are in support of the notion that endogenous SAMHD1 in THP-1 cells forms higher-ordered complexes, which is promoted by the presence of nucleic acids.

When we examined complex formation of wild-type GFP-SAMHD1 and mCherry-SAMHD1 in living cells by FCCS, cross-correlation was close to 30 %. This corresponds to a relative high value when compared to 45 % cross-correlation of a GFP-mCherry fusion protein (data not shown) and taking into account that in a mixture of GFP-SAMHD1 and mCherry-SAMHD1, GFP-SAMHD1/GFP-SAMHD1 and mCherry-SAMHD1/mCherry-SAMHD1 dimers can be formed with the same probability as the mixed coloured dimers. In cells, expressing GFP-SAMHD1-H167Y and mCherry-SAMHD1-H167Y, no cross-correlation was observed (Fig. 4a) indicating that mutation of the catalytic HD-domain renders SAMHD1 incapable of complex formation. In cells transfected with GFP-SAMHD1 alone, the relative brightness was ~2, consistent with an average particle size of at least two monomers, while GFP-SAMHD1-H167Y displayed an average brightness similar to monomeric GFP (Fig. 4b). Thus, within living cells, the most prevalent mobile fraction of wild-type SAMHD1 consists of particles containing two SAMHD1 molecules.

The auto-correlation curves of GFP and SAMHD1-GFP were analysed using a two-component diffusion model (Fig. 4c; Supplementary Methods). As expected for a single diffusing species, monomeric GFP displayed a fast fraction of more than 97 % with a diffusion time of 710±370 μs. For wild-type GFP-SAMHD1, a fast and a slow fraction could be distinguished. The diffusion time of the fast fraction was 1,390±700 μs, which was 1.96 times slower than that of free GFP. As a GFP-SAMHD1 dimer (2×99.1 kDa) would diffuse 1.95 times slower than monomeric GFP (26.9 kDa) under the assumption of globular molecules, the fast diffusing component describes the wild-type GFP-SAMHD1 dimer. In contrast, diffusion of the fast fraction of GFP-SAMHD1-H167Y was significantly faster compared to wild type GFP-SAMHD1 indicating impaired dimerization (Fig. 4c). To quantitatively compare the slow diffusing components, we reanalysed the auto-correlation curves using fixed fast diffusing times corresponding to a dimer (1,390 μs, 1.95 times GFP) for wild-type GFP-SAMHD1 and a monomer (1,090 μs, 1.54 times GFP) for GFP-SAMHD1-H167Y, respectively. As shown in Fig. 4d, e, GFP-SAMHD1-H167Y harboured a significantly reduced slow fraction compared to wild type GFP-SAMHD1, consistent with impaired oligomerisation.

AGS-associated mutations of SAMHD1 interfere with nuclear targeting

Wild-type GFP-SAMHD1 localized within the nucleus. GFP-SAMHD1-H167Y and GFP-SAMHD1-R290H partially mislocalized in the cytosol, while GFP-SAMHD1-Q548X was persistently distributed both in the nucleus and in the cytosol (Fig. 5a). ΔSAM showed an exclusive cytosolic distribution, whereas SAM properly targeted to the nucleus (Fig. 5a). Thus, while the SAM domain of SAMHD1 is dispensable both for nucleic acid-binding and oligomerisation, it is required for nuclear targeting.

SAMHD1 in cells of AGS patients is unstable

In fibroblasts from the AGS patient, compound heterozygous for R290H and Q548X, SAMHD1 protein was absent. Similarly, SAMHD1 was undetectable in lymphoblastoid cells of this patient, while a weak band of the expected size of 72 kDa could be observed in cells from the patient homozygous for H167Y (Fig. 5c). SAMHD1-mRNA in lymphoblastoid cells was reduced by 48 % in the patient carrying R290H and Q548X, while it was similar to wild-type cells in the patient homozygous for H167Y (Supplementary Figure S4). Thus, the absence of SAMHD1 protein is due to degradation of unstable SAMHD1 protein in the homozygous patient, while in the compound heterozygous patient it is most likely also caused by nonsense-mediated decay of mRNA transcribed from the Q548X allele.

Discussion

SAMHD1 degrades dNTPs, the building blocks of DNA synthesis [1, 19], indicating a role in nucleic acid metabolism. Mutations of SAMHD1 cause AGS which features signs of the autoimmune disease SLE [8]. Both disorders are characterized by activation of the antiviral IFN-α axis [20, 21]. Indeed, inappropriate activation of an IFN-α-mediated innate immune response triggered by recognition of self-nucleic acids is regarded as a central mechanism in lupus pathogenesis [21]. Here we show that SAMHD1 interacts with single-stranded nucleic acids and forms complexes of higher order providing further insight into SAMHD1 function. Our observations are in agreement with a recent study that identified SAMHD1 as a nucleic acid-binding protein using an affinity-based proteomic approach with phosphorothioate DNA and poly (I:C), a synthetic dsRNA analogue, as bait [22]. In contrast to this study, we do not find interaction of SAMHD1 with short blunt-end dsRNA, although we cannot exclude that SAMHD1 may also interact with long dsRNA or with partially dsRNA such as RNA hairpins. The positive cross-correlation between SAMHD1 and nucleic acids in cell lysates indicates that the two molecule species are components of a same mobile complex. Although this may also be explained by the presence of additional yet unknown molecules within the complex, which mediate this association, a direct interaction is confirmed by the positive FRET signal between GFP-SAMHD1 and fluorescently labelled nucleic acids in situ and by pull down of endogenous SAMHD1 from THP-1 cells using biotinylated oligonucleotides.

We show that the SAM domain is not required for nucleic acid binding as a deletion mutant lacking the SAM domain can still fully interact with both ssRNA and ssDNA. Consistent with previous findings [22], we also demonstrate that the nucleic acid-binding region includes the catalytic HD domain as H167Y cannot bind nucleic acids. The observation that Q548X, which lacks the last 78 amino acids, but still carries an intact HD domain, has lost nucleic acid-binding capacity, implicates that the C-terminal end of SAMHD1 is also required for nucleic acid binding. Interestingly, the highly conserved C terminus of SAMHD1 harbours sequences that are necessary for Vpx-dependent recruitment of SAMHD1 to the E3 ubiquitin ligase complex CRL4-DCAF1 and its subsequent proteasomal degradation [23–25]. Our findings suggest that this process may be modulated by interaction of the C terminus of SAMHD1 with nucleic acids possibly of retroviral origin.

By FCCS, we demonstrate that in cell lysates, SAMHD1 forms complexes of higher order corresponding to an average size of eight molecules. However, insight into the precise molecular configuration of these complexes requires further investigation. Oligomerisation does not depend on the SAM domain since deletion of the SAM domain does not interfere with complex formation. Interestingly, while the deletion mutant lacking the SAM domain, but capable of nucleic acid-binding, can still oligomerise, all AGS-associated mutations that have lost the ability to interact with nucleic acids are oligomerisation incompetent. Consistent with this, cells from AGS patients show decreased levels of SAMHD1 protein, supporting the conclusion that loss of complex formation and impaired nucleic-acid binding renders mutant SAMHD1 protein unstable. In addition, decreased SAMHD1 protein may also be due to nonsense-mediated decay as shown for Q548X. Our gel filtration data on THP-1 cell lysates further support complex formation of endogenous SAMHD1. Moreover, complex formation is promoted by the presence of nucleic acids, since removal of nucleic acids by benzonase impedes complex formation.

While the SAM domain region of SAMHD1 is dispensable for both the interaction with nucleic acids and oligomerisation, it is important for subcellular targeting. A deletion mutant lacking the HD domain shows preserved nuclear localization, while the deletion mutant lacking the SAM domain is exclusively cytosolic in distribution. This is in line with recent studies providing evidence for a nuclear localization signal within the N-terminal region preceding the SAM domain [26,

Fig. 2 Association of nucleic acids with SAMHD1 visualized by FCCS. ▶ **a** Background- and crosstalk-corrected auto- and cross-correlation curves of GFP-SAMHD1 with ssRNA and dsRNA, respectively, and of monomeric GFP with ssRNA. Each graph depicts the auto-correlation curves for GFP-SAMHD1 (*cyan*, right *y*-axis) and the TAMRA-labelled oligonucleotide (*magenta*, left *y*-axis) as well as the cross-correlation curve (*blue*, left *y*-axis). The average amplitude of the auto-correlation curve for the TAMRA-labelled oligonucleotide (*magenta*) was ten times lower than the amplitude of GFP-SAMHD1 (*cyan*) indicating a 10-fold molar excess of the oligonucleotide. The high cross-correlation amplitude between GFP-SAMHD1 and ssRNA indicates a strong interaction. A cross-correlation of ~50 % means that ~50 % of all GFP-SAMHD1 molecules bound an ssRNA molecule. Low cross-correlation amplitudes indicate absent interaction between GFP-SAMHD1 and dsRNA or between monomeric GFP and ssRNA, respectively. **b** FCCS analysis reveals a high amount of cross-correlation of wild-type GFP-SAMHD1 (*open bars*) with ssRNA and ssDNA, but not with dsRNA, dsDNA or RNA/DNA hybrids. The "T" indicates which strand of the hybrid was labelled with TAMRA. GFP (*dark grey bars*) alone does not show any cross-correlation with nucleic acids. Differences in cross-correlation of GFP-SAMHD1 with ssRNA and ssDNA compared to GFP alone were significant with $p<0.001$ and $p<0.01$, respectively, by unpaired Student's *t* test. **c** Endogenous SAMHD1 from THP-1 cells is pulled-down by ssRNA and ssDNA, but not by double-stranded oligonucleotides. **d** Schematic of the SAMHD1 peptide, the AGS mutations (H167Y, R290H, Q548X) and two deletion mutants (SAM: GFP-SAMHD1$_{1–130}$; ΔSAM: GFP-SAMHD1$_{111–626}$) examined. **e** Cross-correlation of the AGS-associated mutations or the SAM mutant with ssRNA (*light grey bars*) or ssDNA (*dark grey bars*), respectively, is significantly decreased. Cross-correlation of the ΔSAM mutant with ssRNA and ssDNA is similar to that of wild-type SAMHD1 (WT). Differences in cross-correlation of wild-type GFP-SAMHD1 with ssRNA and ssDNA compared to mutant GFP-SAMHD1, with the exception of ΔSAM, were significant with *p* values ranging from $p<0.001$ to $p<0.01$, respectively (Student's *t* test). Indicated are the means of three independent experiments±SD

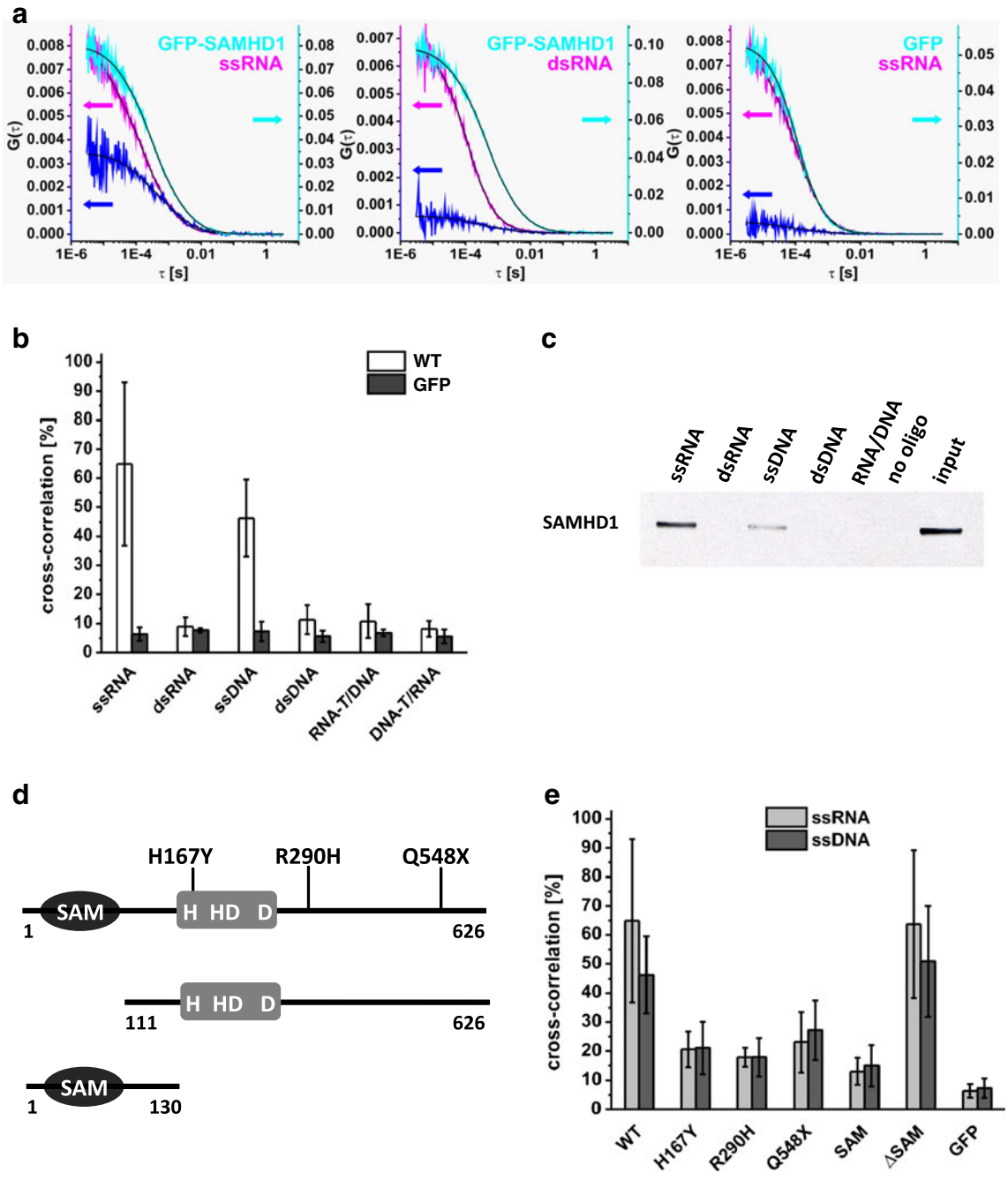

27]. However, partial impairment of nuclear targeting of the AGS-associated SAMHD1 mutations, all of which harbour an intact SAM domain, indicates that subcellular targeting is also influenced by the overall structural integrity of SAMHD1. Collectively, our findings suggest that the properties of SAMHD1 to bind single-stranded nucleic acids and to oligomerise are mutually dependent. This also implies that an impaired interaction of SAMHD1 with nucleic acids may be relevant to AGS pathogenesis.

Intriguingly, H167Y, which affects the first histidine of the catalytic site, abolishes interaction with nucleic acids. This raises the possibility that binding of ssRNA or ssDNA to SAMHD1 could influence enzyme activity by inducing conformational changes that modulate substrate affinity or the allosteric control by dGTP. Notably, dGTP constitutes the most underrepresented dNTP and comprises just 5–10 % of the total dNTP pool, and an increase of dGTP has been shown to correlate with replication errors [28, 29]. Since SAMHD1 is a dGTP-dependent dNTP degrading enzyme, this could argue for a role of SAMHD1 in genome stability. In this scenario, the nucleic acid targets of SAMHD1 may be cell cycle-specific RNA transcripts and DNA intermediates that form

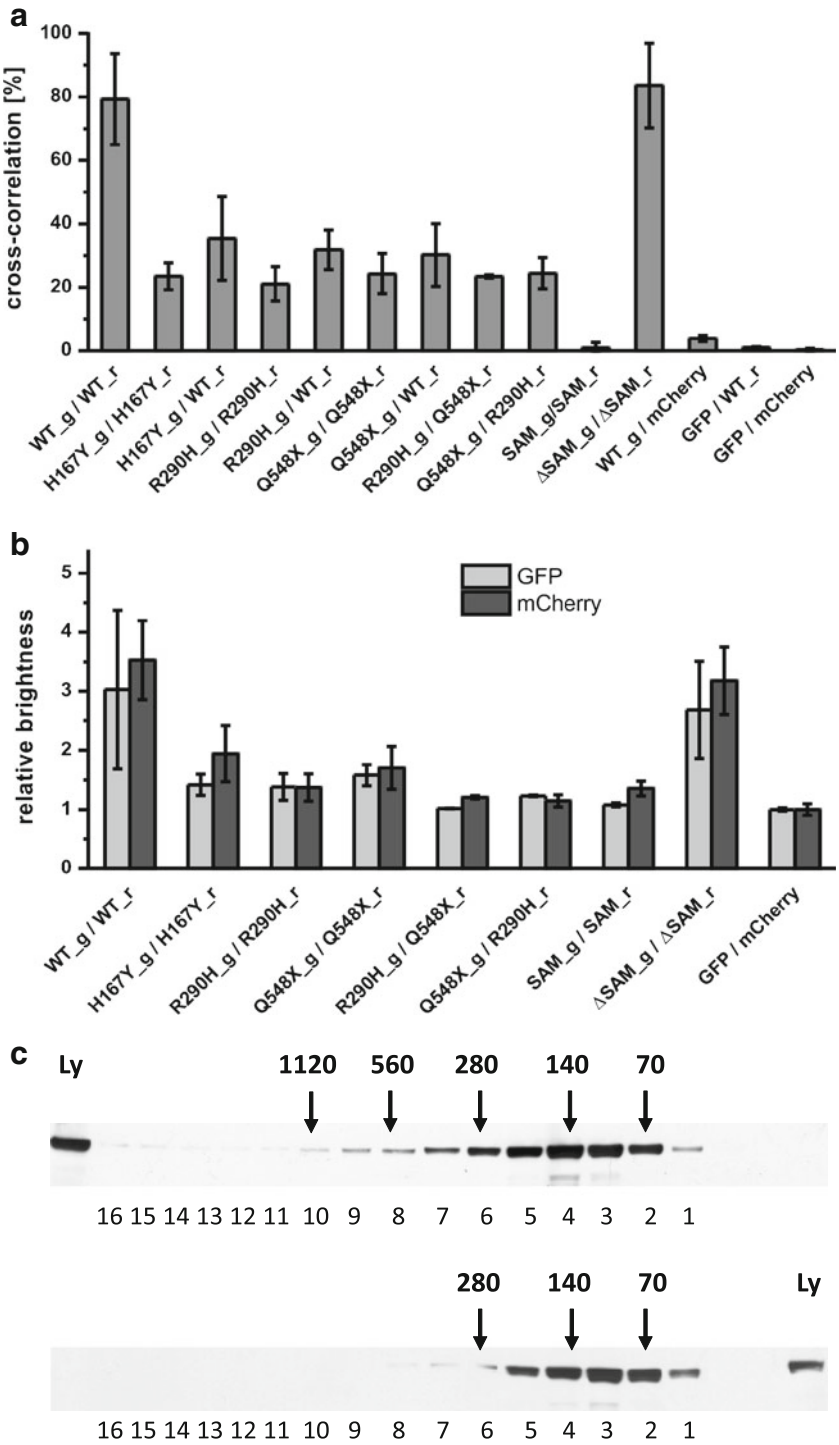

Fig. 3 Complex formation of SAMHD1 in cell lysates. **a** Cross-correlation for the indicated combinations of GFP (_g) and mCherry (_r)-labelled wild type (WT) and SAMHD1 mutants. Shown are the means of at least three experiments±SD. When compared to wild-type complexes, the cross-correlations observed for all hetero- and homozygous combinations of the AGS mutants differ significantly with a value of $p<0.001$ (unpaired Student's *t* test). SAM: GFP-SAMHD1$_{1–130}$; ΔSAM: GFP-SAMHD1$_{111–626}$. **b** Brightness analysis of the fluorescence signal from both fluorescence channels. For GFP and mCherry the mean relative brightness, normalized to the brightness of a single GFP or mCherry molecule±SD is shown. The brightness values for mCherry were corrected for a dark fraction of 55 % (see Supplementary Methods). A value higher than 1 indicates that the average particle of a given measurement is the indicated times brighter than a single fluorescent GFP or mCherry molecule. **c** Gel filtration chromatography of THP-1 cell lysate in absence (*upper*) or presence (*lower*) of benzonase. Numbers of eluted fractions are indicated *below* each blot. Fractions were analysed by SDS-PAGE followed by Western blot using anti-SAMHD1 antibody. The predicted elution positions of the apparent masses corresponding to SAMHD1 complexes with one (~70 kDa), two (~140 kDa), four (~280 kDa), eight (~560 kDa) and 16 (~1120 kDa) molecules are indicated by *arrows*. The molecular weight was estimated from a calibration curve based on the elution volume of standards. *Ly* lysate before fractionation

during DNA replication and repair. It is of interest in this context that RNase H2 functions at sites of genome replication and repair [30, 31]. In keeping with this notion is the recent description of an AGS patient carrying a homozygous SAMHD1 deletion, who presented with multiple deletions of mitochondrial DNA, a phenotype typically observed in inborn errors of mitochondrial dNTP metabolism [32].

Oligomerisation is an integral functional aspect of a many nucleic acid-binding proteins. Recognition of target DNA sequences by p53 is achieved through tetramer formation [33]. Likewise, assembly of replication factors or ribonucleoprotein components into oligomeric complexes is often initiated by binding to nucleic acids [34, 35]. In contrast to the finding of higher-ordered complexes in cell

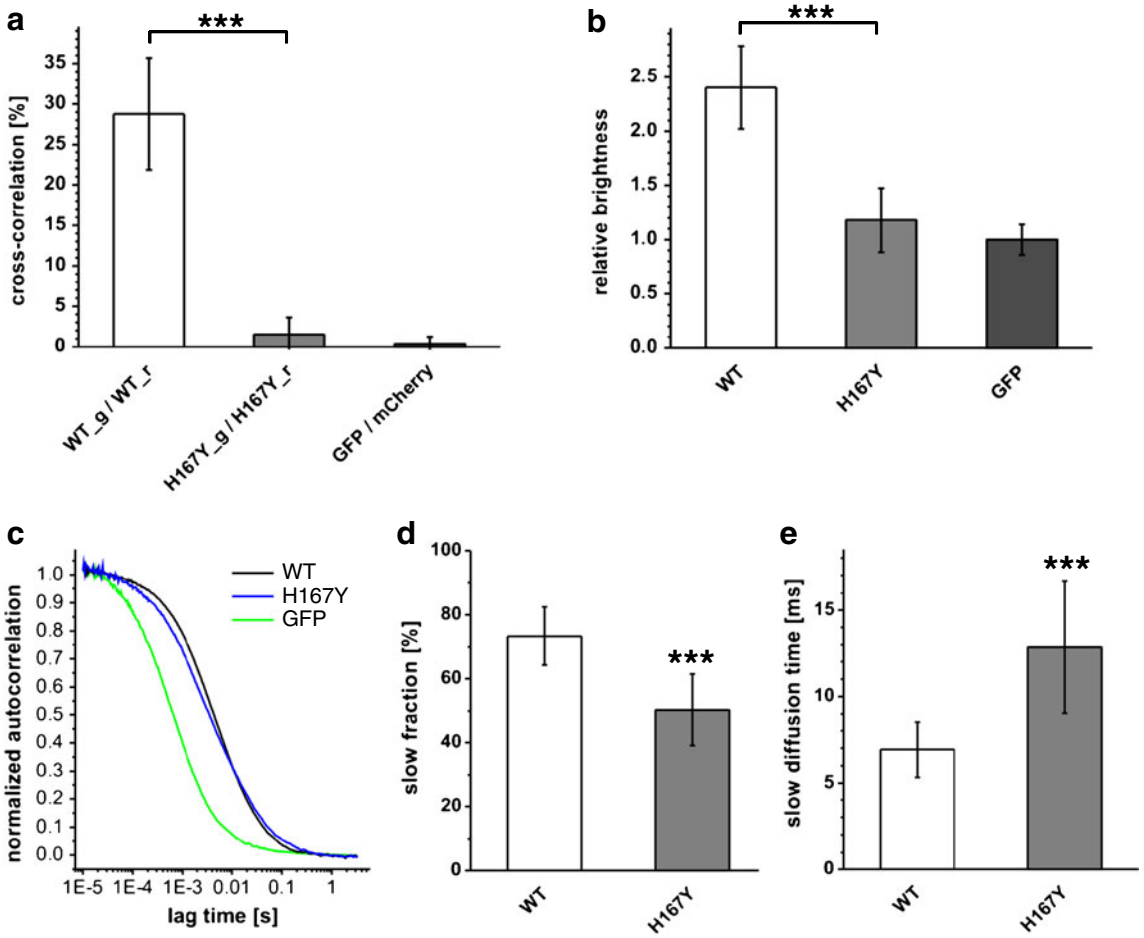

Fig. 4 Complex formation of SAMHD1 in living cells. **a** Cross-correlation of GFP (_g) and mCherry (_r)-labelled wild type (WT) and H167Y mutant. Shown are the means of at least 20 different cells measured in three independent experiments±SD. **b** Brightness analysis of the green fluorescence signal measured in GFP-SAMHD1 transfected cells. Shown is the mean relative brightness, normalized to the brightness of a single GFP molecule, of at least 19 cells measured in two independent experiments±SD. **c** Averaged and normalized autocorrelation curves of GFP, wild-type GFP-SAMHD1 and H167Y mutant. **d**, **e** Rate and diffusion time of the slow fractions of wild-type and mutant GFP-SAMHD1. Shown are the means for at least 17 cells measured in two independent experiments±SD. ***$p<0.001$, unpaired Student's *t* test

lysates, live-cell FCCS revealed that within the intact nuclear environment of living cells, the mobile fraction of wild-type SAMHD1 consists mostly of dimers. This is consistent with previous data showing that recombinant SAMHD1 adopts a dimeric configuration in a concentration-dependent manner [1]. As FCCS measures diffusing particles, only mobile particles contribute to the FCCS signal, while particles bound to nucleic acids within the chromatin will not be captured by FCCS. This is consistent with the finding of a reduced fraction of slow diffusing particles containing H167Y. The increase in diffusion time of this slow fraction in living cells may possibly reflect an association with other molecules or a modification of mutant SAMHD1 that could be involved in protein degradation. The observation of SAMHD1 immunoreactivity in gel filtration fractions of very high mass raises the possibility that multiple SAMHD1 dimers could co-assemble on single-stranded nucleic acid segments. Thus, one may speculate that the SAMHD1 dimer may represent a stable intermediate form able to form complexes of higher order by binding single-stranded DNA or RNA. Although the exact structural nature of SAMHD1 complexes requires further investigation, our findings provide a possible explanation of how nucleic acid binding could impact complex formation and, thus, SAMHD1 function.

SAMHD1 has been shown to down-regulate the dNTP pool required for reverse transcription of the HIV-1 genome [2] implicating SAMHD1 in defence mechanisms against retroviral infection. However, absence of viral infection is a cardinal feature of AGS suggesting a cell-intrinsic source for activation of an innate immune response. Given the role of TREX1 in restriction of endogenous retroelements [36], one

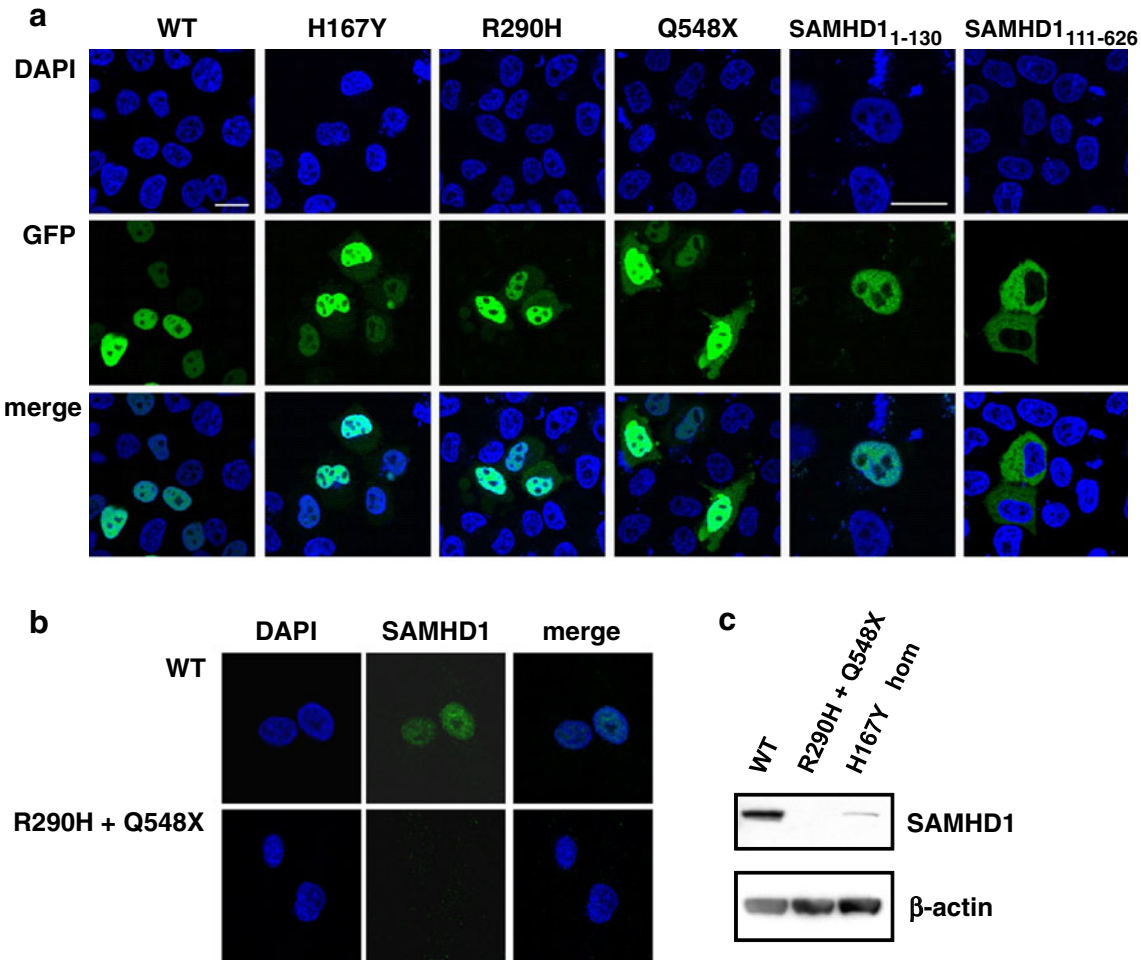

Fig. 5 Subcellular targeting of SAMHD1 is altered by AGS mutations. **a** Nuclear localization of wild-type GFP-SAMHD1 (WT) expressed in HeLa cells is partially impaired in cells expressing the substitution mutations H167Y and R290H, respectively, while the deletion mutant Q548X is consistently distributed both within the nucleus and the cytosol. **b** Nuclear expression of endogenous SAMHD1 protein in wild-type fibroblasts (WT) is absent in fibroblasts from the AGS patient with compound heterozygosity for R290H and Q548X. **c** Western blot analysis of lymphoblastoid cells from two AGS patients shows absent (Q548+R290H) or markedly reduced (H167Y hom) expression of SAMHD1 consistent with complex instability

may also speculate that the nucleic targets of SAMHD1 may originate from retroelements.

The mammalian dNTP supply is regulated by an intricate network of enzymes responsible for synthesis and degradation of dNTPs. Imbalances in the dNTP pool can have genotoxic consequences [37]. SAMHD1 represents a cellular defence against dNTP imbalances by limiting the dNTP supply available for DNA synthesis. Hence, SAMHD1 deficiency could contribute to aberrant synthesis of nucleic acid species that trigger an immune response (Supplementary Figure S5). Our findings establish that SAMHD1 function is tightly regulated by its interaction with single-stranded nucleic acids. The elucidation of the endogenous nucleic acid targets of SAMHD1 is expected to shed more light on the physiological functions of this enzyme and to provide further insight into pathogenic mechanisms underlying activation of the innate immune system in SAMHD1 deficiency.[1]

Acknowledgments We wish to thank Susan Hunger and Kerstin Engel for excellent technical assistance. We are grateful to Barbara Borgonovo (Max Planck Institute of Molecular Cell Biology and Genetics, Dresden) for assistance with gel filtration chromatography and Zdenek Petrasek (Max Planck Institute of Biochemistry, Martinsried) for help with deriving the brightness correction formula. We thank Roger Y. Tsien (University of California, San Diego) for pRSET-mCherry. This work was supported by the Deutsche Forschungsgemeinschaft (KFO 249; LE 1074/4-1 to M.L.-K., KFO 249; SCHW 716/12-1 to P.S.) and a MeDDrive grant (60.283 to B.K.).

[1] While this manuscript was in review, a paper by White et al. reported binding of SAMHD1 to phosphorothioate-modified DNA [38].

Conflicts of interest The authors declare no conflicts of interest.

References

1. Goldstone DC, Ennis-Adeniran V, Hedden JJ, Groom HC, Rice GI, Christodoulou E, Walker PA, Kelly G, Haire LF, Yap MW et al (2011) HIV-1 restriction factor SAMHD1 is a deoxynucleoside triphosphate triphosphohydrolase. Nature 480:379–382
2. Lahouassa H, Daddacha W, Hofmann H, Ayinde D, Logue EC, Dragin L, Bloch N, Maudet C, Bertrand M, Gramberg T et al (2012) SAMHD1 restricts the replication of human immunodeficiency virus type 1 by depleting the intracellular pool of deoxynucleoside triphosphates. Nat Immunol 13:223–228
3. Hrecka K, Hao C, Gierszewska M, Swanson SK, Kesik-Brodacka M, Srivastava S, Florens L, Washburn MP, Skowronski J (2011) Vpx relieves inhibition of HIV-1 infection of macrophages mediated by the SAMHD1 protein. Nature 474:658–661
4. Laguette N, Sobhian B, Casartelli N, Ringeard M, Chable-Bessia C, Segeral E, Yatim A, Emiliani S, Schwartz O, Benkirane M (2011) SAMHD1 is the dendritic- and myeloid-cell-specific HIV-1 restriction factor counteracted by Vpx. Nature 474:654–657
5. Rice GI, Bond J, Asipu A, Brunette RL, Manfield IW, Carr IM, Fuller JC, Jackson RM, Lamb T, Briggs TA et al (2009) Mutations involved in Aicardi–Goutieres syndrome implicate SAMHD1 as regulator of the innate immune response. Nat Genet 41:829–832
6. Crow YJ, Hayward BE, Parmar R, Robins P, Leitch A, Ali M, Black DN, van Bokhoven H, Brunner HG, Hamel BC et al (2006) Mutations in the gene encoding the 3′–5′ DNA exonuclease TREX1 cause Aicardi–Goutieres syndrome at the AGS1 locus. Nat Genet 38:917–920
7. Crow YJ, Leitch A, Hayward BE, Garner A, Parmar R, Griffith E, Ali M, Semple C, Aicardi J, Babul-Hirji R et al (2006) Mutations in genes encoding ribonuclease H2 subunits cause Aicardi–Goutieres syndrome and mimic congenital viral brain infection. Nat Genet 38:910–916
8. Ramantani G, Kohlhase J, Hertzberg C, Innes AM, Engel K, Hunger S, Borozdin W, Mah JK, Ungerath K, Walkenhorst H et al (2010) Expanding the phenotypic spectrum of lupus erythematosus in Aicardi–Goutieres syndrome. Arthritis Rheum 62:1469–1477
9. Ramantani G, Hausler M, Niggemann P, Wessling B, Guttmann H, Mull M, Tenbrock K, Lee-Kirsch MA (2011) Aicardi–Goutieres syndrome and systemic lupus erythematosus (SLE) in a 12-year-old boy with SAMHD1 mutations. J Child Neurol 26:1425–1428
10. Ravenscroft JC, Suri M, Rice GI, Szynkiewicz M, Crow YJ (2011) Autosomal dominant inheritance of a heterozygous mutation in SAMHD1 causing familial chilblain lupus. Am J Med Genet A 155A:235–237
11. Rice G, Newman WG, Dean J, Patrick T, Parmar R, Flintoff K, Robins P, Harvey S, Hollis T, O'hara A et al (2007) Heterozygous mutations in trex1 cause familial chilblain lupus and dominant Aicardi–Goutieres syndrome. Am J Hum Genet 80:811–815
12. Lee-Kirsch MA, Chowdhury D, Harvey S, Gong M, Senenko L, Engel K, Pfeiffer C, Hollis T, Gahr M, Perrino FW et al (2007) A mutation in TREX1 that impairs susceptibility to granzyme A-mediated cell death underlies familial chilblain lupus. J Mol Med 85:531–537
13. Lee-Kirsch MA, Gong M, Chowdhury D, Senenko L, Engel K, Lee YA, de Silva U, Bailey SL, Witte T, Vyse TJ et al (2007) Mutations in the gene encoding the 3′–5′ DNA exonuclease TREX1 are associated with systemic lupus erythematosus. Nat Genet 39:1065–1067
14. Lorenz M (2009) Visualizing protein–RNA interactions inside cells by fluorescence resonance energy transfer. RNA 15:97–103
15. Schwille P, Meyer-Almes FJ, Rigler R (1997) Dual-color fluorescence cross-correlation spectroscopy for multicomponent diffusional analysis in solution. Biophys J 72:1878–1886
16. Bacia K, Kim SA, Schwille P (2006) Fluorescence cross-correlation spectroscopy in living cells. Nat Methods 3:83–89
17. Foo YH, Naredi-Rainer N, Lamb DC, Ahmed S, Wohland T (2012) Factors affecting the quantification of biomolecular interactions by fluorescence cross-correlation spectroscopy. Biophys J 102:1174–1183
18. Padilla-Parra S, Auduge N, Lalucque H, Mevel JC, Coppey-Moisan M, Tramier M (2009) Quantitative comparison of different fluorescent protein couples for fast FRET-FLIM acquisition. Biophys J 97:2368–2376
19. Powell RD, Holland PJ, Hollis T, Perrino FW (2011) Aicardi–Goutieres syndrome gene and HIV-1 restriction factor SAMHD1 is a dGTP-regulated deoxynucleotide triphosphohydrolase. J Biol Chem 286:43596–43600
20. Lebon P, Badoual J, Ponsot G, Goutieres F, Hemeury-Cukier F, Aicardi J (1988) Intrathecal synthesis of interferon-alpha in infants with progressive familial encephalopathy. J Neurol Sci 84:201–208
21. Marshak-Rothstein A (2006) Toll-like receptors in systemic autoimmune disease. Nat Rev Immunol 6:823–835
22. Goncalves A, Karayel E, Rice GI, Bennett KL, Crow YJ, Superti-Furga G and Burckstummer T (2012) SAMHD1 is a nucleic-acid binding protein that is mislocalized due to Aicardi–Goutieres syndrome-associated mutations. Hum Mutat 33:1116–1122
23. Ahn J, Hao C, Yan J, Delucia M, Mehrens J, Wang C, Gronenborn AM, Skowronski J (2012) HIV/simian immunodeficiency virus (SIV) accessory virulence factor Vpx loads the host cell restriction factor SAMHD1 onto the E3 ubiquitin ligase complex CRL4DCAF1. J Biol Chem 287:12550–12558
24. Laguette N, Rahm N, Sobhian B, Chable-Bessia C, Munch J, Snoeck J, Sauter D, Switzer WM, Heneine W, Kirchhoff F et al (2012) Evolutionary and functional analyses of the interaction between the myeloid restriction factor SAMHD1 and the lentiviral Vpx protein. Cell Host Microbe 11:205–217
25. Lim ES, Fregoso OI, McCoy CO, Matsen FA, Malik HS, Emerman M (2012) The ability of primate lentiviruses to degrade the monocyte restriction factor SAMHD1 preceded the birth of the viral accessory protein Vpx. Cell Host Microbe 11:194–204
26. Brandariz-Nunez A, Valle-Casuso JC, White TE, Laguette N, Benkirane M, Brojatsch J, Diaz-Griffero F (2012) Role of SAMHD1 nuclear localization in restriction of HIV-1 and SIVmac. Retrovirology 9:49
27. Wei W, Guo H, Han X, Liu X, Zhou X, Zhang W and Yu XF (2012) A novel DCAF1-binding motif required for Vpx-mediated degradation of nuclear SAMHD1 and Vpr-induced G2 arrest. Cell Microbiol 14:1745–1756
28. Zhang X, Mathews CK (1995) Natural DNA precursor pool asymmetry and base sequence context as determinants of replication fidelity. J Biol Chem 270:8401–8404
29. Martomo SA, Mathews CK (2002) Effects of biological DNA precursor pool asymmetry upon accuracy of DNA replication in vitro. Mutat Res 499:197–211
30. Bubeck D, Reijns MA, Graham SC, Astell KR, Jones EY, Jackson AP (2011) PCNA directs type 2 RNase H activity on DNA replication and repair substrates. Nucleic Acids Res 39:3652–3666
31. Nick McElhinny SA, Kumar D, Clark AB, Watt DL, Watts BE, Lundstrom EB, Johansson E, Chabes A, Kunkel TA (2010) Genome instability due to ribonucleotide incorporation into DNA. Nat Chem Biol 6:774–781
32. Leshinsky-Silver E, Malinger G, Ben-Sira L, Kidron D, Cohen S, Inbar S, Bezaleli T, Levine A, Vinkler C, Lev D et al (2011) A large homozygous deletion in the SAMHD1 gene causes atypical

Aicardi–Goutieres syndrome associated with mtDNA deletions. Eur J Hum Genet 19:287–292
33. McLure KG, Lee PW (1998) How p53 binds DNA as a tetramer. EMBO J 17:3342–3350
34. Mott ML, Erzberger JP, Coons MM, Berger JM (2008) Structural synergy and molecular crosstalk between bacterial helicase loaders and replication initiators. Cell 135:623–634
35. Collins BM, Cubeddu L, Naidoo N, Harrop SJ, Kornfeld GD, Dawes IW, Curmi PM, Mabbutt BC (2003) Homomeric ring assemblies of eukaryotic Sm proteins have affinity for both RNA and DNA. Crystal structure of an oligomeric complex of yeast SmF. J Biol Chem 278:17291–17298
36. Stetson DB, Ko JS, Heidmann T, Medzhitov R (2008) Trex1 prevents cell-intrinsic initiation of autoimmunity. Cell 134:587–598
37. Mathews CK (2006) DNA precursor metabolism and genomic stability. FASEB J 20:1300–1314
38. White TE, Brandariz-Nuñez A, Carlos Valle-Casuso J, Amie S, Nguyen L, Kim B, Brojatsch J, Diaz-Griffero F (2012) Contribution of SAM and HD domains to retroviral restriction mediated by human SAMHD1. Virology. doi:10.1016/j.virol.2012.10.029